Prediction of meteorological drought in arid and semi-arid regions using PDSI and SDSM: a case study in Fars Province, Iran

Sheida DEHGHAN[1], Nasrin SALEHNIA[2], Nasrin SAYARI[1*], Bahram BAKHTIARI[1]

[1] Department of Water Engineering, Faculty of Agriculture, Shahid Bahonar University of Kerman, Kerman 7616914111, Iran;
[2] Faculty of Agriculture, Ferdowsi University of Mashhad, Mashhad 9177949207, Iran

Abstract: Drought is one of the most significant environmental disasters, especially in arid and semi-arid regions. Drought indices as a tool for management practices seeking to deal with the drought phenomenon are widely used around the world. One of these indicators is the Palmer drought severity index (PDSI), which is used in many parts of the world to assess the drought situation and continuation. In this study, the drought state of Fars Province in Iran was evaluated by using the PDSI over 1995–2014 according to meteorological data from six weather stations in the province. A statistical downscaling model (SDSM) was used to apply the output results of the general circulation model in Fars Province. To implement data processing and prediction of climate data, a statistical period 1995–2014 was considered as the monitoring period, and a statistical period 2019–2048 was for the prediction period. The results revealed that there is a good agreement between the simulated precipitation (R^2>0.63; R^2, determination coefficient; MAE<0.52; MAE, mean absolute error; RMSE<0.56; RMSE, Root Mean Squared Error) and temperature (R^2>0.95, MAE<1.74, and RMSE<1.78) with the observed data from the stations. The results of the drought monitoring model presented that dry periods would increase over the next three decades as compared to the historical data. The studies showed the highest drought in the meteorological stations Abadeh and Lar during the prediction period under two future scenarios representative concentration pathways (RCP4.5 and RCP8.5). According to the results of the validation periods and efficiency criteria, we suggest that the SDSM is a proper tool for predicting drought in arid and semi-arid regions.

Keywords: PDSI; SDSM; RCP4.5; RCP8.5; climate change; extreme drought

1 Introduction

One of the critical subjects facing the world is climate change since it is predicted to alter climate patterns and increase the frequency of extreme weather events (Palmer and Raisanen, 2002; Hayes et al., 2004; IPCC, 2012). Over the last few years, the frequency of droughts caused by global warming-related climate change has increased and along with an increase in the intensity of these events (IPCC, 2013; Yu et al., 2013; Salehnia et al., 2017a). Therefore, it is crucial to establish appropriate expectations of future drought impacts of severe droughts caused by the

---

*Corresponding author: Nasrin SAYARI (Email: nasrin_sayari@yahoo.com)

Received 2019-02-14; revised 2019-11-11; accepted 2020-01-25

climate change. This study investigates the impact of climate change on drought over a long-term scale, which is necessary to diminish vulnerability and establish suitable innovation strategies for drought mitigation and preparedness. Drought is a significant natural stochastic hazard that arises from a considerable deficiency in precipitation (Gao and Zhang, 2016), which can have devastating impacts on the regional agriculture, water resources and environment (Sternberg, 2011; Escalante-Sandoval and Nuñez-Garcia, 2017, Salehnia et al., 2017b), causing extensive damage and affect a large number of people. Droughts and floods are extreme climate events that percentage-wise are likely to change more rapidly than the mean climate (Trenberth et al., 2003). With increasing temperature and changing distribution of precipitation, the drought risk is expected to rise further (Sillmann et al., 2013).

The most important index in the meteorological drought is the Palmer drought severity index (PDSI), which was developed by Palmer in 1965. The PDSI can be used to measure the cumulative variation compared to local mean conditions in atmospheric moisture supply and demand at the ground surface; and to simulate the moisture content of the soil in monthly scale and compare its anomalies in regions under different climatic conditions (Szép et al., 2005). The PDSI might be the most extensively used regional drought index for observing droughts (Alley, 1984). However, the PSDI introduced as a meteorological drought index based on soil moisture content and meteorological variables. It counts several conditions, such as precipitation, evapotranspiration and soil moisture (Alley, 1984). The PDSI can be used to determine the beginning, ending and severity of the drought periods, and has been normalized to allow comparisons across space and time.

The PDSI is traditionally calculated using a two-layer bucket type model to obtain water balance components, which does not consider the impacts of spatial heterogeneity of soil, vegetation cover and topography on watershed hydrological processes, etc. (Jin et al., 2016). In previous studies, the PDSI was estimated mostly based on the meteorological station monitoring at point scale and having the restriction of collecting long-term serial soil moisture and actual evapotranspiration at a large scale. Additionally, the PDSI in the previous studies could not precisely reflect the regional differentiation of drought. Moreover, the PDSI uses a simplified model of potential evaporation, which only responds to the changes in temperature and thus responds incorrectly to global warming in recent decades (Sheffield et al., 2012). These indices have been used extensively to detect long-term drought trends under global warming in some areas around the world. According to the findings, drought phenomena have been increasing around the world because of climate change in the past few decades (Dai, 2011, 2013). A global climate model (GCM) is generally used for predicting long-term drought by projecting meteorological and hydrological data and applying different future climate scenarios (Hessami et al., 2007). Considerable studies are published based on climate change models and future climate scenarios presenting significant changes in occurrence and duration of severe drought (Dai, 2013; Bak and Labedzki, 2014; Dubrovský et al., 2014; Touma et al., 2015). The fifth evaluation report carried out by the Intergovernmental Panel for Climate Change (IPCC) introduced the representative concentration pathway (RCP) to achieve much more accurate forecasting of future climate (Moss et al., 2010).

The objective of this study was to find out the trend of drought under climate change conditions using the PDSI in Fars Province of Iran under two future scenarios RCP4.5 and RCP8.5. It would be in help for understanding and predicting drought trends in the arid and semi-arid regions around the world.

2 Study area and methods

2.1 Study area

The study area, Fars Province (27°03′–31°40′N, 50°36′–55°33′E), is located in the southwest of Iran, covering an area of 1.33×10^5 km^2 (Fig. 1). The study area can be divided into three categories according to its climatic characteristics: the north and northwest part with cold winter

and mild summer, the south and southeast part with cold winter and hot summer, and the central area with rainy, mild winter and hot, dry summer (Rahimi et al., 2013).

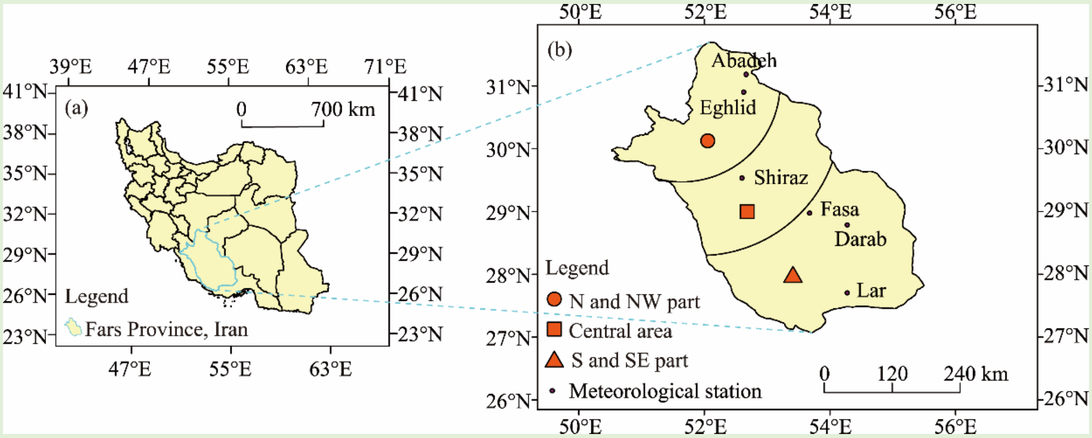

Fig. 1 Location of the study area, Fars Province of Iran (a). The north and northwest part has cold winter and mild summer; the central has rainy, mild winter and hot, dry summer; and the south and southeast part has cold winter and hot summer (b). N, north; NW, northwest; S, south, SE, southeast.

Historical daily weather data of six different locations across the study area were collected from the meteorological stations, Shiraz, Fasa, Abadeh, Darab, Lar and Eghlid (Fig. 1). Physiographic details of the six stations are presented in Table 1.

Table 1 Characteristics of the six meteorological stations in Fars Province of Iran during 1995–2014

Meteorological station	Location	Elevation (m)	Mean annual temperature (°C)	Total daily precipitation (mm)	Climate
Shiraz	29°32′N, 52°36′E	1484	18.6	6370.1	Semi-arid
Fasa	28°58′N, 53°41′E	1288	19.4	5429.3	Semi-arid
Abadeh	31°11′N, 52°40′E	2030	14.4	2649.4	Arid
Darab	28°47′N, 54°17′E	1098	22.1	4983.8	Arid
Lar	27°42′N, 54°17′E	792	23.9	3533.2	Arid
Eghlid	30°54′N, 52°38′E	2300	13.0	6325.9	Arid

2.2 Data

The observed data covered the period 1995–2014, which was used as the baseline period. Daily meteorological variables, including daily average temperature and total daily precipitation, were used to calculate the drought indices. In this study, a range of future climate change scenarios were presented by the IPCC. The representative concentration pathways form a set of greenhouse gas concentration and emission pathways that are designed to support researches on impacts and potential policy responses to climate change (Moss et al., 2010). The data, which included two types of daily predictors needed for this research, were obtained from the Canadian Institute for Climate Studies (CICS) website (http://www.cics.uvic.ca/scenar ios/sdsm/select.cgi), including 26 predictors of the national center of environmental prediction (NCEP) and 26 predictors of Canadian Earth System Model (CanESM2) under RCP4.5 and RCP8.5 scenarios for the period 2019–2048. The CanESM2 under RCP output data was input to the calibrated statistical downscaling model (SDSM) for each meteorological station to reproduce future daily temperature and precipitation values.

For better analyzing, the boxplot diagram is applied in the result section. In this kind of plot, the altitude of the box expresses the interquartile range (IQR, i.e., 25th–75th quantiles), the horizontal line inward the box shows the group median (black line), the multiply sign refers to the

mean value, and the vertical lines (called whiskers) exporting from the box extend to the group minimum and maximum values.

2.3 Modification of PDSI

Palmer (1965) developed the PDSI and combined antecedent precipitation, moisture supply and moisture demand into a hydrologic accounting system. The PDSI has been widely used as a reasonable comparable local significance both in space and time for drought measurement and water resources management.

2.3.1 Concepts and necessary steps for the PDSI calculation

The PDSI is based on the water balance equation. The difference between the actual precipitation (*P*) and climatically appropriate for existing conditions precipitation ($\hat{P}$) is an indicator of water deficiency or surplus, which can be expressed as Equations 1 and 2.

$$d = P - \hat{P}\,, \tag{1}$$

$$\hat{P} = \mathrm{ET} + R + \mathrm{RO} - L\,, \tag{2}$$

where *d* is the moisture departure (mm); ET is the evapotranspiration (mm); *R* is the recharge of soil moisture (mm); RO is the runoff (mm); and *L* is the loss of soil moisture (mm).

2.3.2 Drought severity

The *d* (mm) is the excess or shortage of precipitation compared to the climatically appropriate for existing conditions precipitation. Necessarily, the same *d* is interpreted differently at different times and locations. This procedure prevents straightforward comparisons to be made between different values of *d*. For correction of this aspect, the moisture departure is weighted using *K*, which is called the climatic characteristic. Here, *K* is a refinement of *K*′, which is Palmer's general estimation for the climate parameter of a location. Palmer derived Equations 3 and 4 for *K*′ and *K*, respectively.

$$K_i' = 1.5 \times \log_{10}\left(\frac{\dfrac{\overline{\mathrm{PET}_i} + \overline{R_i} + \overline{\mathrm{RO}_i}}{\overline{L_i} + \overline{P_i}} + 2.5}{\overline{D_i}}\right) + 0.5\,, \tag{3}$$

where K_i' was a weighting factor for the *i* month; $\overline{\mathrm{PET}_i}$, $\overline{R_i}$, $\overline{\mathrm{RO}_i}$, $\overline{L_i}$, $\overline{P_i}$ and $\overline{D_i}$ were the potential evapotranspiration (mm), soil water recharge (mm), runoff (mm), loss of soil moisture (mm), precipitation (mm) and average soil moisture departure (mm) at the i^{th} month, respectively. The parameter (($\overline{\mathrm{PET}_i} + \overline{R_i} + \overline{\mathrm{RO}_i}$)/($\overline{L_i} + \overline{P_i}$)) was a measure of the ratio of moisture demand to moisture supply at the i^{th} month for the region.

$$K_i = \frac{17.67}{\sum_{i=1}^{12} \overline{D_i} K_i'} K_i'\,, \tag{4}$$

where the value of 17.67 was an empirical constant that Palmer derived using data from nine different locations in seven states of the United States (Palmer 1965). Weighting factor K_i tends to be large in arid regions and small in humid areas. During the derivation of K_i, Palmer (1965) assumed that the economic consequences of the driest year in one place were the same as those of the driest year in other places. The influence of large-scale changes in water usage, such as those resulting from reservoir development, urbanization, or changes in irrigation practices, is ignored.

The purpose of the climatic characteristic, K_i, is to adjust the value of *d* according to the characteristics of the climate in such a way as to allow for accurate comparisons of PDSI values over time and space. The value of $\overline{D_i}$ was computed from Equation 5:

$$\bar{D}_i = \frac{\sum_{\text{all year}} |d_i|}{\#\text{of years in record}}. \tag{5}$$

The result of multiplying d (the moisture departure) by K is called the moisture anomaly index, Z index (Eq. 6).

$$Z = d \times K. \tag{6}$$

The Z index can be used to show how wet or dry it was during a single month without regarding to the recent precipitation trends. The Z index is used to calculate the PDSI value for a given month using Equation 7.

$$X_{3i} = 0.897 X_{3i-1} + Z_i / 3, \tag{7}$$

where X refers to the drought severity for calculating the PDSI; X_{3i}, X_{3i-1} and Z_i are the PDSI and Z index values for the i^{th} month. For example, to estimate the current value of X_{3i}, 0.897 times the previous PDSI value, X_{3i-1} is added to 1/3 of the present moisture anomaly Z_i. Palmer called the values 0.897 and 1/3 as the duration factors. Palmer derived them empirically from two locations, the western Kansas and central Iowa in the US, which are affected by the sensitivity of the index to precipitation events. According to Palmer's recommendation, the monthly time series range is between –4.00 and 4.00 (Table 2), where the negative (positive) values of the index indicate dry (wet) periods; moreover, the values close to zero have a climatic condition similar to the standard conditions of the area. For computing the PDSI, the drought monitor and prediction tool (AgrimetSoft, 2018) was applied in this research.

Table 2 Drought classification by PDSI value

PDSI value	Classification
≥4.00	Extreme wet
3.00–3.99	Very wet
2.00–2.99	Moderate wet
1.00–1.99	Slight wet
0.50–0.99	Incipient wet spell
0.49– –0.49	Near normal
–0.50– –0.99	Incipient dry spell
–1.00– –1.99	Mild drought
–2.00– –2.99	Moderate drought
–3.00– –3.99	Severe drought
≤–4.00	Extreme drought

Note: PDSI, Palmer drought severity index.

2.4 Description of the statistical downscaling model (SDSM)

Wilby et al. (2002) developed the SDSM, which is a combination of the multiple linear regression and stochastic weather generator. The SDSM, NCEP, and GCM generated 100 daily time series predictors to fit closely with the observed data during the validation period. As the standard, twenty-time series are considered when the other studies used the similar sets as well (Wilby et al., 2002; Chu et al., 2010). There are two sub-models, including unconditional and conditional, that are used according to the requirement of the predictands. For instance, independent parameters like temperature are applied in the unconditional sub-model, while dependent parameters such as precipitation are involved in the conditional sub-model (Wilby et al., 2002; Ashiq et al., 2010). Figure 2 shows the general scheme of the SDSM framework for generating climate scenario information. On the occurrence of an event, the model process can be conditional (i.e., for precipitation) or unconditional (i.e., for temperature).

2.4.1 Screening of predictors

The most crucial process in statistical downscaling is the screening of large scale variables (Wilby

et al., 2002; Huang et al., 2011). Different indicators can be used for this purpose. In this study, a combination of the correlation matrix, partial correlation and *P*-value was used. The same combination was also used by Huang et al. (2011), and Mahmood and Babel (2013).

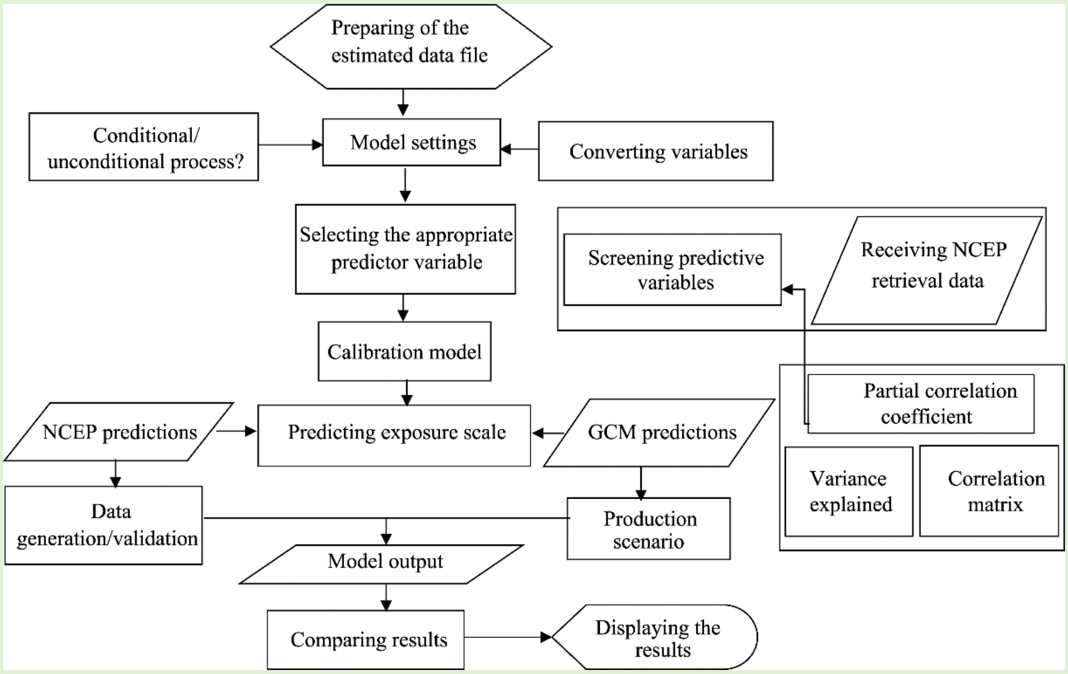

Fig. 2 Flowchart of estimating climate variables through the statistical downscaling model (SDSM). NCEP, national center of environmental prediction; GCM, global climate model.

2.4.2 Calibration and validation

After the calibration, the model needs to be evaluated. Root mean square error (RMSE), mean absolute error (MAE), and Nash and Sutcliffe efficiency (NSE) were applied to assess and compare the accuracy of the methods and scenarios of the model used and to identify the best way for predicting temperature and precipitation. In the present study, two performance indicators, the coefficient of determination (R^2; Eq. 8) and RMSE, were used for validation period (Wang et al., 2012). The accuracy of the model was computed for each station. Then, the mean values of each index were obtained from all the stations. Many researchers, e.g., Ashiq et al. (2010), Chu et al. (2010) and Wang et al. (2012), also used the SDSM to observe the variations and patterns.

$$R^2 = \frac{\left(\sum_{i=1}^{n}\left[O_i - \overline{O}_i\right]\left[P_i - \overline{P}_i\right]\right)^2}{\sum_{i=1}^{n}\left[O_i - \overline{O}_i\right]^2 \sum_{i=1}^{n}\left[P_i - \overline{P}_i\right]^2}, \tag{8}$$

$$\mathrm{RMSE} = \sqrt{\frac{\sum_{i=1}^{n}\left(O_i - P_i\right)^2}{n}}, \tag{9}$$

$$\mathrm{MAE} = \frac{\sum_{i=1}^{n}\left|O_i - P_i\right|}{n}, \tag{10}$$

$$\mathrm{NSE}=1-\frac{\sum_{i=1}^{n}\left(O_i-P_i\right)^2}{\sum_{i=1}^{n}\left(O_i-\bar{O}_i\right)^2}, \tag{11}$$

where O_i was the observation value and P_i was the prediction or modeled value. $\overline{O_i}$ and $\overline{P_i}$ were the average observed and predicted or modeled values, respectively.

2.5 Inverse Distance Weighted (IDW) method for zoning

There is an excellent range of methods and techniques available for data interpolation or zoning. The main characteristic of this method is that all the points on the Earth's surface are considered to be interdependent on the basis of distance. IDW interpolation defines cell values using a weighted combination of a set of sample points. The weight is a function of the inverse distance (Achilleos, 2011). In this research, the IDW method was run through the ArcGIS 10.2 software and the second-order IDW method.

3 Results and discussion

3.1 SDSM calibration and validation

To run the SDSM, we calibrated the connection between predictands and predictors before future climate situation with GCM outputs could be effectively downscaled. Precipitation and temperature data were used for calibration and validation. The R^2 between daily simulated and observed temperatures exceeded 0.90, and precipitation exceeded 0.60 in the validation period 2019–2033 (Table 3). In order to clarify the model capability, the statistical criteria (R^2, RMSE, MAE and NSE) were also used. The lower the RMSE and MAE values and the higher the NSE, the more efficient the model. According to Table 3, the scenarios in evaluating the precipitation rate of the Eghlid station and in estimating the temperature of the Shiraz station were more efficient and more accurate than other stations. These results showed that there was a good accord between the simulated precipitation and temperature data and the observed data.

Table 3 Results of the model evaluation in the validation period 2019–2033

Meteorological station	Precipitation				Temperature			
	R^2	RMSE	MAE	NSE	R^2	RMSE	MAE	NSE
Shiraz	0.89	0.39	0.19	0.80	0.99	0.44	0.37	0.99
Fasa	0.63	0.50	0.36	0.65	0.99	1.14	0.98	0.99
Abadeh	0.66	0.21	0.15	0.61	0.97	1.42	0.70	0.97
Darab	0.71	0.36	0.23	0.75	0.95	1.78	1.74	0.95
Lar	0.75	0.56	0.52	0.64	0.99	0.52	0.45	0.99
Eghlid	0.93	0.13	0.14	0.97	0.96	1.42	1.14	0.96

Note: R^2, determination coefficient; RMSE, root mean square error; MAE, mean absolute error; NSE, Nash and Sutcliff efficiency.

3.2 Drought prediction for 2019–2048 under RCP4.5 and RCP8.5 scenarios

The results showed that the monthly precipitation variables of Fars Province would generally increase under different scenarios during the future period 2019–2048 (Fig. 3). In January to March, July, August and November, extreme precipitation decreases at Eaghlid, Abadeh, Shiraz, Darab and Lar, but increases in Fasa. In February, April, May, September and December, precipitation is increasing in Darab, Lar, Fasa, Eghlid and Shiraz but decreasing in Abadeh. However, in September, precipitation decreases at most stations. Generally, the simulated monthly average precipitation in all stations under both scenarios will increase for the future period. The temperature value will decrease in February, March, April and May at Fasa; in June, July, August, September, October and November at Eghlid; and in April and May at LAR.

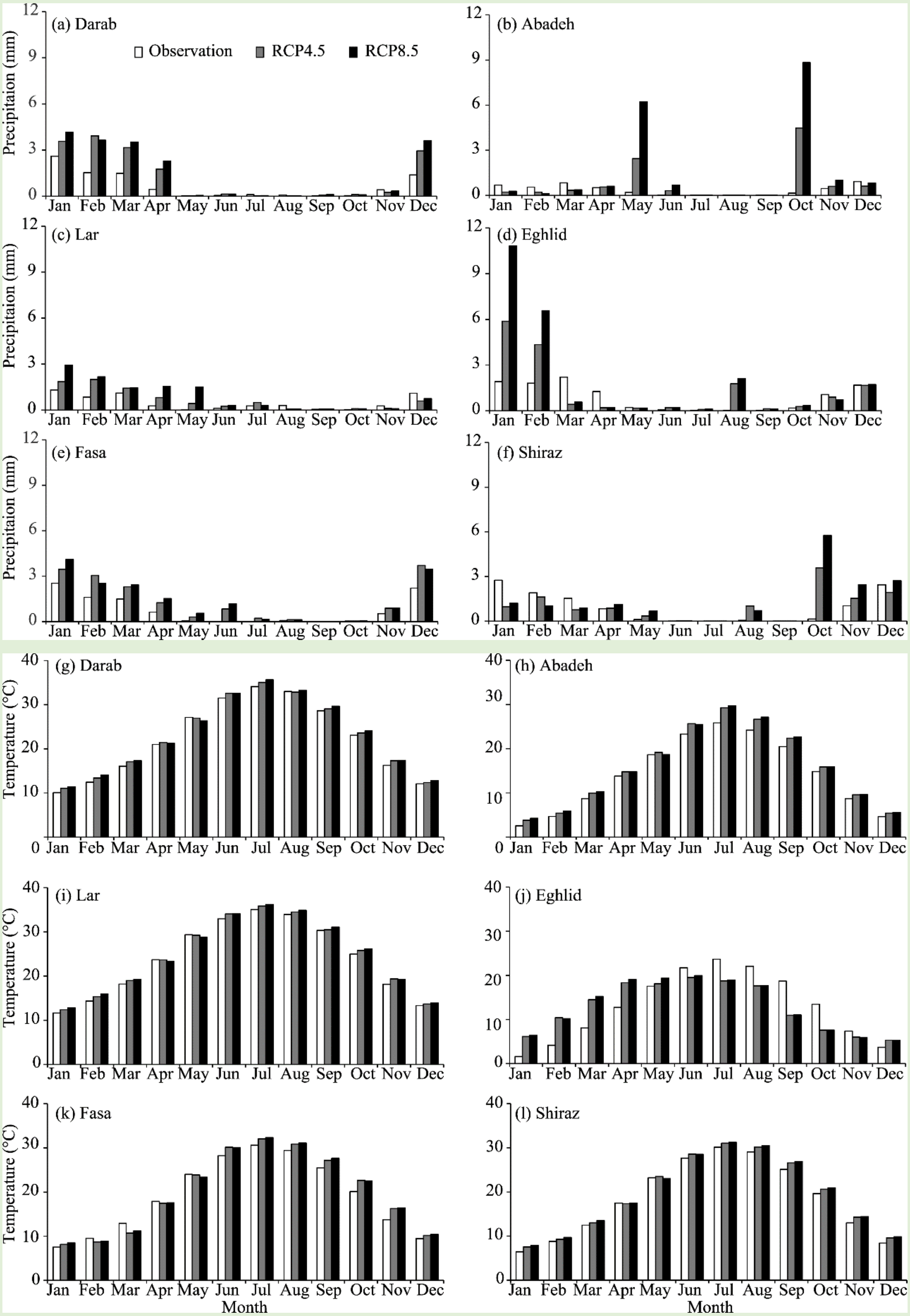

Fig. 3 Observed (1995–2014) and simulated (2019–2048) maximum monthly precipitation (a–f) and monthly average temperature (g–l) under RCP4.5 and RCP8.5 scenarios at selected stations of Fars Province, Iran

However, in both scenarios, the temperature will increase in the other months at Fasa, Eghlid, Lar and Darab, and in all the months at Abadeh and Shiraz. Moreover, under RCP8.5, the incremental amount in the average temperature changes is higher than those under other scenarios (Vallam and Qin, 2017). The results could be attributed to the fact that greenhouse gas emissions and other negative impacts are higher under RCP8.5 and RCP4.5 scenarios than under the other RCP scenarios (Wu et al., 2016).

3.3 Temporal trends of drought risk under historical drought events

Historical drought events in Fars Province were used to evaluate the precision of the drought indices of this study. According to the drought criteria presented in Tables 2 and 4, extreme droughts happened in Abadeh in 2008, Eghlid in 2000 and 2008, Shiraz in 2008 and 2010, Fasa in 2001 and 2008, Darab in 2001, and Lar in 2000. Compared to the previous years, the precipitation decreased significantly in 2000, 2001, 2008 and 2010. Zandi lak et al. (2014) evaluated the reclamation drought index in Fars Province, which were consistent with the results of our researches (Zandi lak et al., 2014) for the period 1984–2009.

Table 4 Extreme drought events in Fars Province during 1995–2014

Meteorological station	Year	Annual precipitation (mm)	Precipitation of the previous year (mm)
Abadeh	2008	36.3	152.7
Darab	2001	100.0	195.4
Eghlid	2000	232.0	299.0
	2008	123.1	386.2
Fasa	2001	138.2	243.7
	2008	112.5	185.3
Lar	2000	102.1	123.6
Shiraz	2008	125.8	241.7
	2010	94.3	281.0

For the prediction period 2019–2048 (Table 5), under RCP4.5, the highest number of the dry months related to Abadeh over the first, second and third decades were 85, 80 and 82 months, respectively. The lowest were 33 months in the first and 54 months in the third decades at Eghlid. Fasa dedicated with 59 months in the second decade. In the first decade under RCP8.5, the driest period with 69 months were obtained for Lar, and the lowest drought frequency was related to Shiraz, which was 46 months. In the second decade, the driest stations were Fasa and Lar with 88 months. The least observation in this decade belonged to Darab with 57 months. In the third decade of prediction, the highest and the lowest dry months appeared in Abadeh and Eghlid.

Table 5 Number of dry months in the prediction period 2019–2048

Meteorological station	RCP4.5			RCP8.5		
	2039–2048	2029–2038	2019–2028	2039–2048	2029–2038	2019–2028
	(Months)					
Shiraz	75	66	68	46	79	77
Fasa	59	59	64	58	88	66
Abadeh	85	80	82	68	58	101
Darab	58	62	66	63	57	65
Lar	64	75	64	69	88	72
Eghlid	33	67	54	64	65	57

3.4 Monthly PDSI boxplot

The boxplot is a favorable method to present statistical information for analysis. The PDSI values through boxplots of the CanESM2 model under RCP4.5 and RCP8.5 scenarios for 2019–2048 were shown in Figures 4 and 5. According to the results of Table 5, the Abadeh station had the highest number of dry months, so we selected Abadeh for analyzing the drought conditions. The

IQR of the boxplots in both scenarios were not relatively the same and had apparent differences in different parts of the boxplots. The length of IQR under RCP8.5 was higher than that under RCP4.5, especially in summer and autumn. There were noticeable changes in the two scenarios. The median changes of the RCP8.5 indicated the PDSI increased compared to the RCP4.5 over the prediction period 2019–2048. The boxplots showed the maximum value of the PDSI was 7.00 in February and the minimum was –4.00 in November under RCP4.5, whereas the maximum was 9.50 in July and minimum was –4.00 in November under RCP8.5. Further analysis of the PDSI boxplots revealed that the values of drought under RCP8.5 had not been changed in comparison to RCP4.5, whereas the number of wet months (Table 2) was incremental. As shown in Figure 4, in the months of winter and early spring, the IQR was higher than in the other months, denoting that the PDSI value under RCP4.5 in this winter was more marked by changes than in the different seasons. In Figure 5, the IQRs were higher in the summer months than in the other months, indicating that the PDSI value under the RCP8.5 was more significant in summer than in the other seasons.

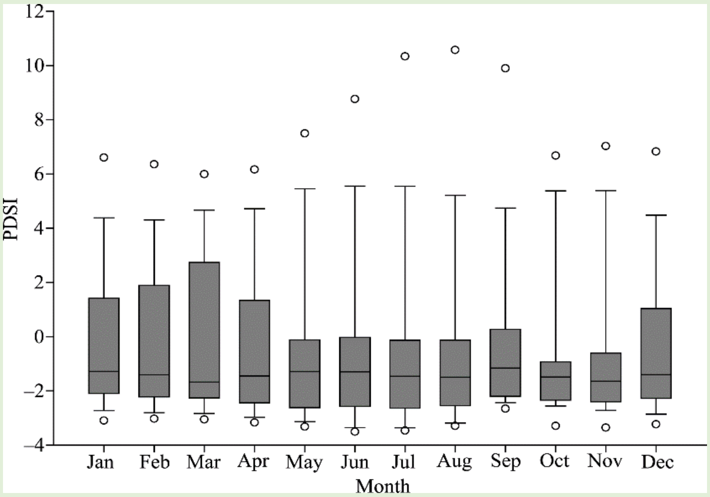

Fig. 4 Boxplot for the monthly Palmer drought severity index (PDSI) at the Abadeh station under RCP4.5 for the prediction period 2019–2048. The horizontal line inward the box shows the group median (black line), and the multiple sign refers to the mean. The circles refer to outlier data.

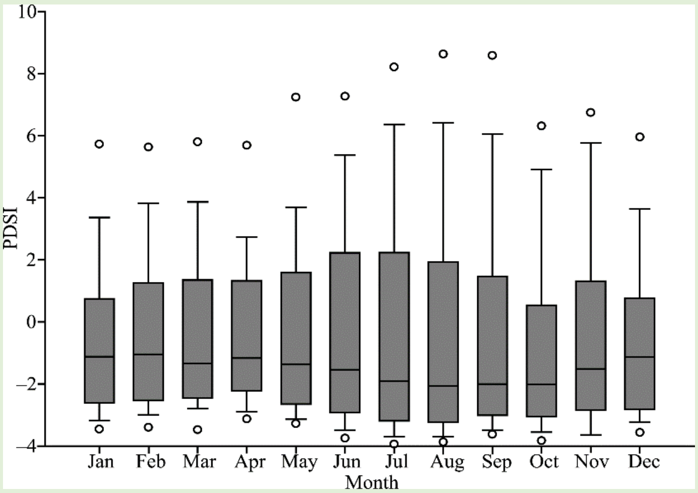

Fig. 5 Boxplot for the monthly Palmer drought severity index (PDSI) at the Abadeh station under RCP8.5 for the prediction period 2019–2048. The horizontal line inward the box shows the group median (black line), and the multiply sign refers to the mean. The circles refer to outlier data.

3.5 PDSI zoning

Because there were only six stations in this study, the results of the ArcGIS 10.2 software and the second-order IDW (Inverse distance weighting) method were used for zoning. The IDW was one of the local interpolation methods (Morid et al., 2006). The three selected months, October 2020, July 2036 and August 2042, for displaying the PDSI were presented in Figures 6 and 7. It should be noted that these three months were exemplary and did not necessarily mean the PDSI of the specified months.

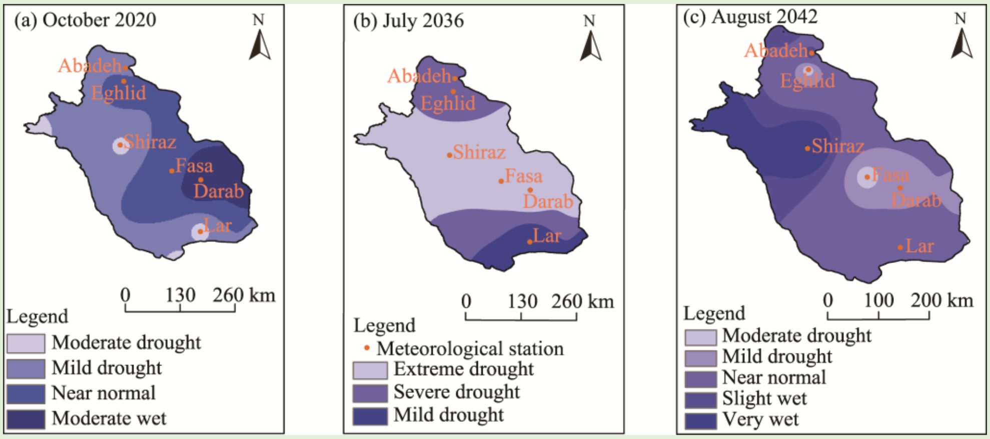

Fig. 6 PDSI values under RCP4.5 during 2019–2048

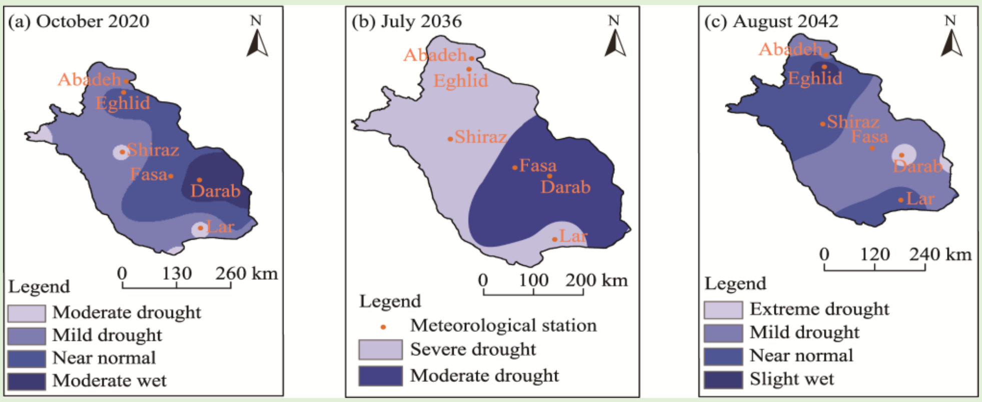

Fig. 7 PDSI values under RCP8.5 during 2019–2048

3.5.1 Results under RCP4.5 during the prediction period 2019–2048

Our investigations showed that under RCP4.5, the first drought period will appear in October 2020 in the first decade of 2019–2028 (Fig. 6a). The study area will experience a dry and mild period in the west. The intensity of the dry periods over the oriental side of the area will decrease. Eventually, the eastern study area will experience a period from the normal to the moderate wet condition. It appears that Darab will likely to be placed on a wet condition, but Shiraz and Lar will be in the early dry period. In July 2036 (Fig. 6b), the 8th year of the second decade (2029–2038), severe drought will be observed in the north; and a very severe drought will happen in the central part. The PDSI shows a moderate to mild drought towards the south. In the 4th year (August 2042) of the third decade (2039–2048), a small part of the north area and part of the southeastern study area will present a moderate to mild drought (Fig. 6c). From the east to west in the study area, the PDSI values indicate a change from normal to wet. Therefore, more than 70% of the study area will experience a normal summer during this prediction period 2019–2048 under RCP4.5 scenario.

3.5.2 Results under RCP8.5 during the prediction period 2019–2048

The first drought period will appear in October 2020 in the first decade 2019–2028 (Fig. 7a),

during which the northern study area will experience a very severe to moderate drought period (Fig. 7a). The intensity of wet periods will decrease in the southern area and eventually, the area will be somewhat dry. Lar will have a dry period 2020–2038. In July 2036 (Fig. 7b), the 8th year of the second decade (2029–2038), the entire study area will be affected by drought, with severe droughts in the north and moderate droughts in the south. In August 2042, the 24th year of the third decade (2039–2048), there will be a severe drought in the east and southeast of the study area (Fig. 7c). Towards the west, the drought will go down slightly. Eghlid will appear to be having a near-wet period. So more than 70% of the study area will experience drought in the summer during this prediction period 2019–2048 under RCP8.5 scenario.

4 Conclusions

With global warming, the durability of drought events will change in the future. It is necessary to assess the characteristics of future drought by using accurate and scientific methods to decrease the negative effects of drought. This is especially important in Iran, which has been exposed to frequent droughts in recent decades. Fars Province is one of the main areas of Iran, where the tourism and agricultural industries have been developed recently. The results of this study show that the dryness rate in the whole Fars Province will intensify in the future with increased temperature and decreased precipitation, which will have a significant negative effects on wheat and other products yield.

This research aims to investigate the effects of climate change on drought through the PDSI in Fars Province of Iran. The periods 1995–2014 and 2019–2048 were selected as the monitoring and prediction periods, respectively. We also applied CanESM2 under RCP4.5 and RCP8.5 scenarios for the prediction of future drought. The results show that: (1) the variation of precipitation and temperature generally increases in different future scenarios; (2) under the SDSM, the mean monthly precipitation decreased and the temperature variable increased in each station; (3) the frequency of drought under the PDSI will increase during the simulated periods compared to the monitoring period (far future>near future>observations); (4) the frequency of wet years under the PDSI in the province will increase during prediction periods compared to the monitoring periods (near future>observation); and (5) the frequency of normal years under the PDSI in the province will increase during the prediction periods compared to the monitoring periods (near future>observation).

Therefore, we suggest that the SDSM simulations is a proper tool for drought prediction in arid and semi-arid regions. The conclusion of this research could be in help with the sustainable water resources and agriculture management and planning.

References

Achilleos G A. 2011. The inverse distance weighted interpolation method and error propagation mechanism–creating a DEM from an analogue topographical map. Journal of Spatial Science, 56(2): 283–304.

Agricultural and Meteorological Software. 2018. Drought monitor and prediction (Version 1.0). [2019-11-10]. https://agrimetsoft.com/Drought Monitoring And Prediction.aspx.

Alley W M. 1984. The Palmer drought severity index: limitations and assumptions. Journal of Applied Meteorology, 23(7): 1100–1109.

Ashiq M W, Zhao C, Ni J, et al. 2010. GIS-based high-resolution spatial interpolation of precipitation in mountain–plain areas of upper Pakistan for regional climate change impact studies. Theoretical and Applied Climatology, 99(3–4): 239.

Bak B, Labedzki L. 2014. Prediction of precipitation deficit and excess in Bydgoszcz Region in view of predicted climate change. Journal of Water and Land Development, 23(1): 11–19.

Chu J T, Xia J, Xu C Y, et al. 2010. Statistical downscaling of daily mean temperature, pan evaporation and precipitation for climate change scenarios in Haihe River, China. Theoretical and Applied Climatology, 99(1–2): 149–161.

Dai A. 2011. Characteristics and trends in various forms of the Palmer Drought Severity Index during 1900–2008. Journal of Geophysical Research: Atmospheres, 116(D12), doi: 10.1029/2010JD015541.

Dai A. 2013. Increasing drought under global warming in observations and models. Nature Climate Change, 3(1): 52–58.

Dubrovský M, Hayes M, Duce P, et al. 2014. Multi-GCM projections of future drought and climate variability indicators for the Mediterranean region. Regional Environmental Change, 14(5): 1907–1919.

Escalante-Sandoval C, Nuñez-Garcia P. 2017. Meteorological drought features in northern and northwestern parts of Mexico

under different climate change scenarios. Journal of Arid Land, 9(1): 65–75.

Hayes M J, Wilhelmi O V, Knutson C L. 2004. Reducing drought risk: bridging theory and practice. Natural Hazards Review, 5(2): 106–113.

Hessami M, Gachon P, Ouarda B M J, et al. 2007. Automated regression-based statistical downscaling tool. Environmental Modelling & Software, 23(6): 813–834.

Huang J, Zhang J, Zhang Z, et al. 2011. Estimation of future precipitation change in the Yangtze River basin by using statistical downscaling method. Stochastic Environmental Research and Risk Assessment, 25(6): 781–792.

Intergovernmental Panel on Climate Change (IPCC). 2012. Managing the risks of extreme events and disasters to advance climate change adaptation. In: Field C B, Barros V, Stocker T F, et al. A Special Report of Working Groups I and II of the Intergovernmental Panel on Climate Change. Cambridge: Cambridge University Press, 115.

IPCC. 2013. Climate change 2013: the physical science basis. In: Stocker T F, Qin D, Plattner M, et al. An Overview of the Working Group I Contribution to the Fifth Assessment Report of the Intergovernmental Panel on Climate Change. Cambridge: Cambridge University Press, 112.

Jin J, Wang Q, Li L H. 2016. Long-term oscillation of drought conditions in the western China: an analysis of PDSI on a decadal scale. Journal of Arid Land, 8(6): 819–831.

Gao L M, Zhang Y N. 2016. Spatio-temporal variation of hydrological drought under climate change during the period 1960–2013 in the Hexi Corridor, China. Journal of Arid Land, 8(2): 157–171.

Mahmood R, Babel M. 2013. Evaluation of SDSM developed by annual and monthly sub-models for downscaling temperature and precipitation in the Jhelum basin, Pakistan and India. Theoretical and Applied Climatology, 113(1–2): 27–44.

Morid S, Smakhtin V, Moghaddasi M. 2006. Comparison of seven meteorological indices for drought monitoring in Iran. International Journal of Climatology, 26(7): 971–985.

Moss R H, Edmonds J A, Hibbard K A, et al. 2010. The next generation of scenarios for climate change research and assessment. Nature, 463(7282): 747–756.

Palmer T N, Räisänen J. 2002. Quantifying the risk of extreme seasonal precipitation events in a changing climate. Nature, 415(6871): 512–514.

Palmer W C. 1965. Meteorological Drought. Washington: Office of Climatology, US Weather Bureau, 7–12.

Rahimi J, Ebrahimpour M, Khalili A. 2013. Spatial changes of extended De Martonne climatic zones affected by climate change in Iran. Theoretical and Applied Climatology, 112(3–4), 409–418.

Salehnia N, Zare H, Kolsoumi S, et al. 2017a. Predictive value of Keetch-Byram Drought Index for cereal yields in a semi-arid environment. Theoretical and Applied Climatology, 134: 1005–1014.

Salehnia N, Alizadeh A, Sanaeinejad H, et al 2017b. Estimation of meteorological drought indices based on AgMERRA precipitation data and station-observed precipitation data. Journal of Arid Land, 9(6): 797–809.

Sheffield J, Wood E F, Roderick M L. 2012. Little change in global drought over the past 60 years. Nature, 491(7424): 435–438.

Sillmann J, Kharin V V, Zwiers F W, et al. 2013. Climate extremes indices in the CMIP5 multimodel ensemble: Part 2. Future climate projections. Journal of Geophysical Research: Atmospheres, 118(6): 2473–2493.

Sternberg T. 2011. Regional drought has a global impact. Nature, 472(7342):169–169.

Szép I J, Mika J, Dunkel Z. 2005. Palmer drought severity index as soil moisture indicator: physical interpretation, statistical behaviour and relation to global climate. Physics and Chemistry of the Earth, Parts A/B/C, 30(1–3): 231–243.

Touma, D, Ashfaq M, Nayak M A, et al. 2015. A multi-model and multi–index evaluation of drought characteristics in the 21st century. Journal of Hydrology, 526: 196–207.

Trenberth K E, Dai A, Rasmussen R M, et al. 2003. The changing character of precipitation. American Meteorological Society. [2003-09-01]. https://doi.org/10.1175/BAMS-84-9-1205.

Vallam P, Qin X S. 2017. Projecting future precipitation and temperature at sites with diverse climate through multiple statistical downscaling schemes. Theoretical and Applied Climatology, 134: 669–688.

Wang X Y, Yang T, Shao Q X, et al. 2012. Statistical downscaling of extremes of precipitation and temperature and construction of their future scenarios in an elevated and cold zone. Stochastic Environmental Research and Risk Assessment, 26(3): 405–418.

Wilby R L, Dawson C W, Barrow E M. 2002. SDSM–a decision support tool for the assessment of regional climate change impacts. Environmental Modelling & Software, 17(2): 145–157.

Wu C, Xian Z, Huang G. 2016. Meteorological drought in the Beijiang River basin, South China: current observations and future projections. Stochastic Environmental Research and Risk Assessment, 30(7): 1821–1834.

Yu G, Sauchyn D, Li Y F. 2013. Drought changes and the mechanism analysis for the North American Prairie. Journal of Arid Land, 5(1): 1–14.

Zandi L H, Fooladmand H R, Boustani F. 2014. Evaluation of the wheat agricultural drought return period in the province of Fars using RDI index. Water Engineering, 7(22): 1–10.